

Supporting Information

Band and microstructure engineering toward high thermoelectric performance in SnTe

Jingli Xu¹, Zizhen Zhou^{1,*}, Kaiqi Zhang¹, Ting Zhao¹, Yiqing Wei², Bin Zhang³,
Honghui Wang^{1,*}, Xu Lu^{1,*} and Xiaoyuan Zhou^{1,3}

¹ Chongqing Key Laboratory of Interface Physics in Energy Conversion and College of Physics, Chongqing University, Chongqing 401331, P. R. China

² College of Physics and Electronic Engineering, Chongqing Normal university, Chongqing 401331, P. R. China

³ Analytical and Testing Center, Chongqing University, Chongqing 401331, P. R. China

*Corresponding authors: zzzhou@cqu.edu.cn, wanghh@cqu.edu.cn and luxu@cqu.edu.cn

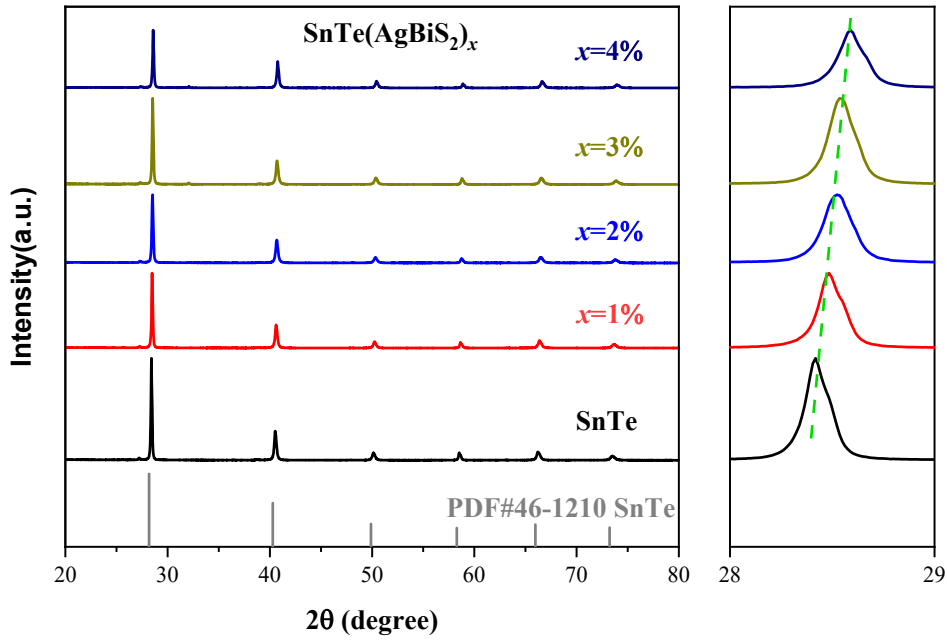


Figure S1 Powder XRD patterns and Enlargement of the powder XRD patterns at 28°~ 29° for all $\text{SnTe}(\text{AgBiS}_2)_x$ ($x = 1\%$, 2% , 3% , and 4%) samples.

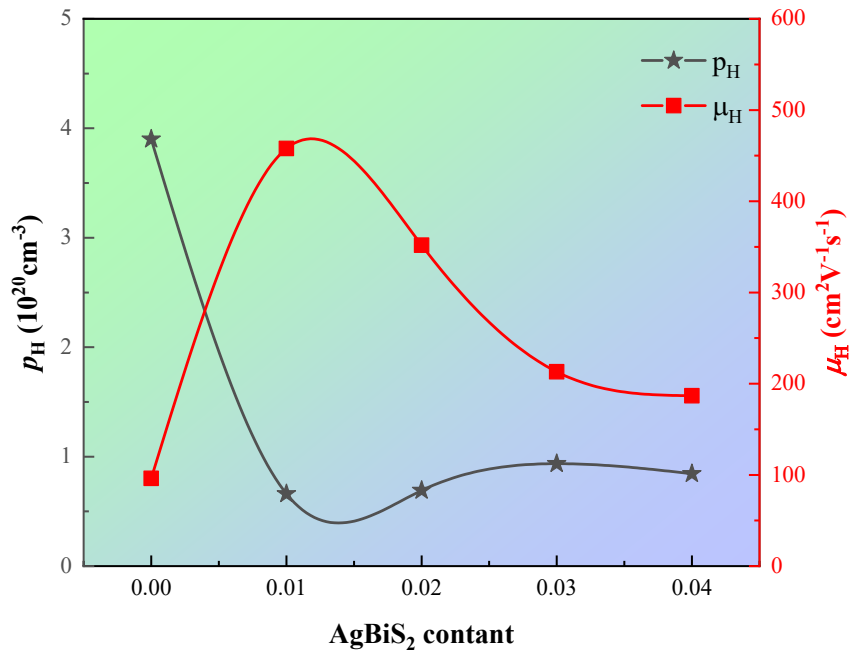


Figure S2 The relationship between Hall carrier concentration and Hall mobility with alloying AgBiS_2 content.

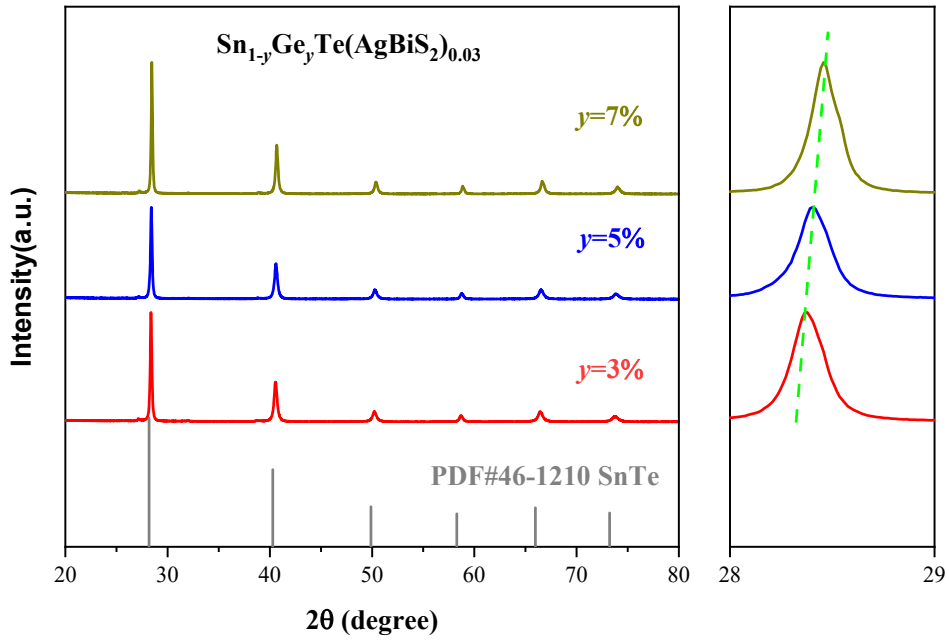


Figure S3 Powder XRD patterns and Enlargement of the powder XRD patterns at $28^\circ \sim 29^\circ$ for all $\text{Sn}_{1-y}\text{Ge}_y\text{Te}(\text{AgBiS}_2)_{0.03}$ ($y = 3\%$, 5% , and 7%) samples.

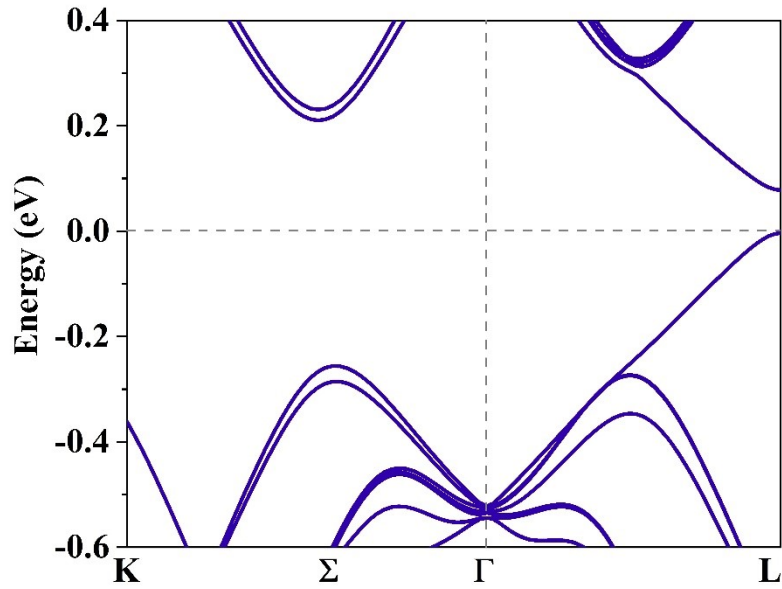


Figure S4 Band structures of Ge doped SnTe.

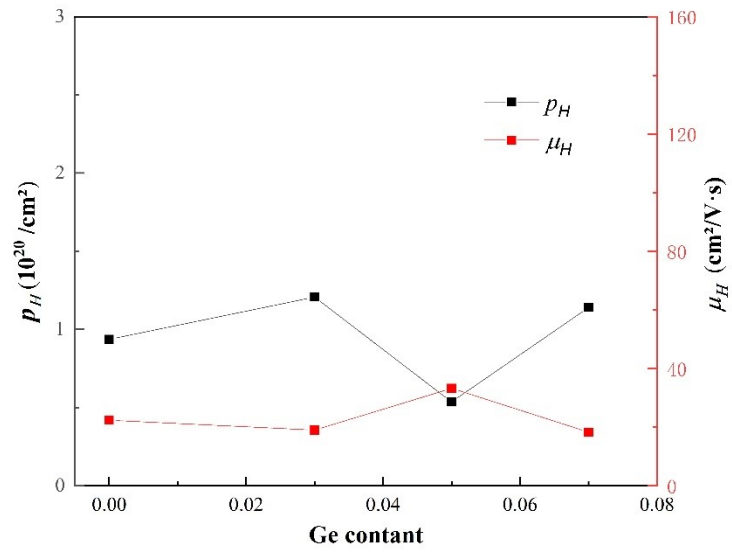


Figure S5 The relationship between Hall carrier concentration and Hall mobility with Ge doping content.

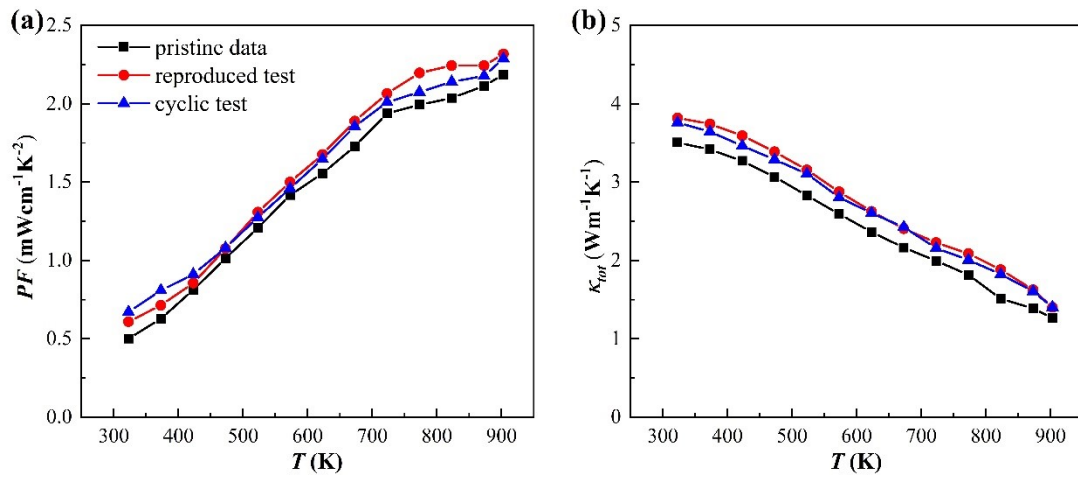


Figure S6 The cycling stability and measurement repeatability tests for the sample with the highest zT values.

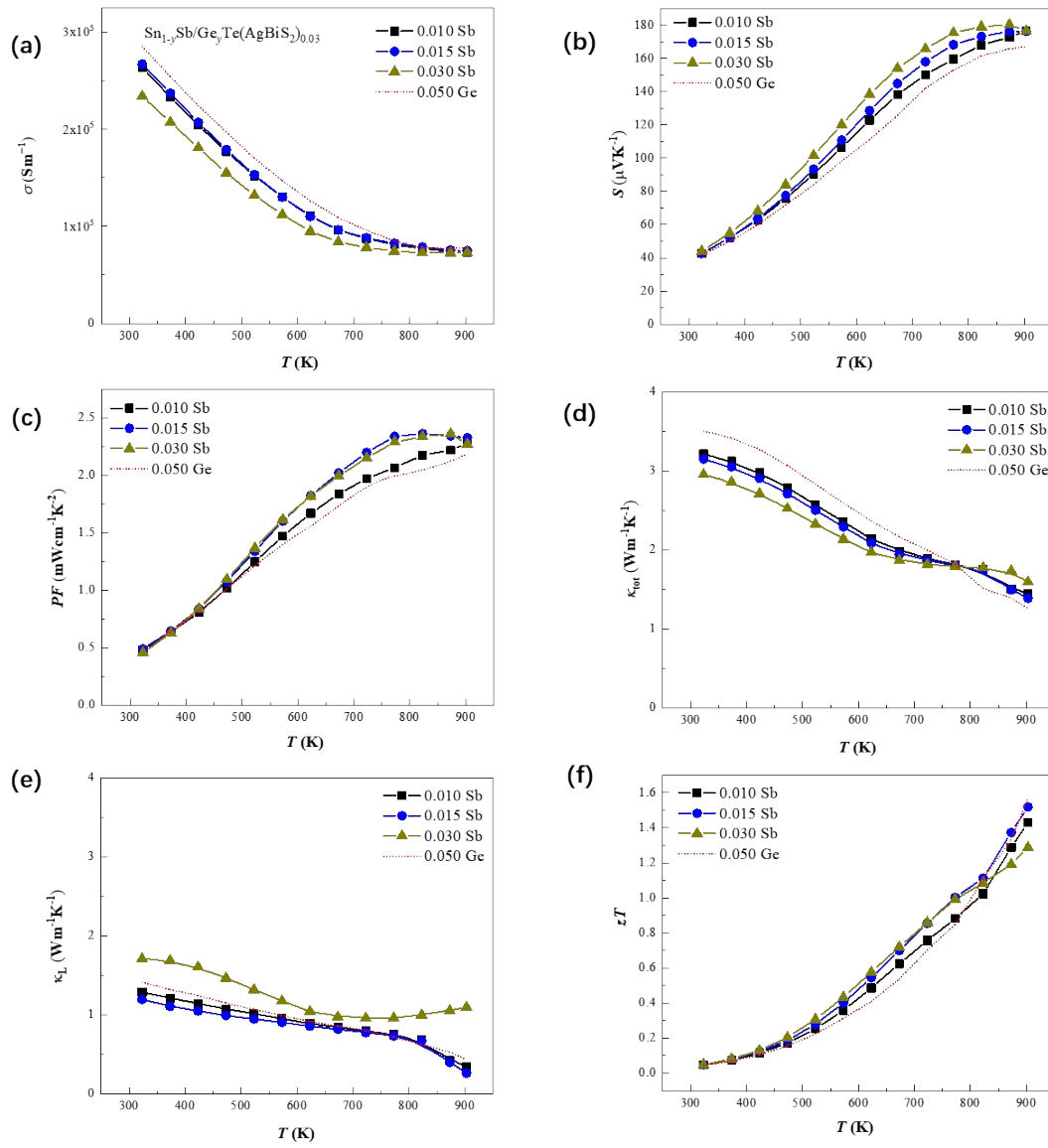


Figure S7 Temperature dependence of (a) electrical conductivity, (b) Seebeck coefficient, (c) power factor, (d) thermal conductivity, (e) lattice thermal conductivity, and (f) zT values of $\text{Sn}_{1-y}\text{Sb}/\text{Ge}_y\text{Te}+0.03\text{AgBiS}_2$ samples.